

Original Article

Pancreatic neuroendocrine neoplasms: a correlative study of imaging characteristics and histological grade

Lei Meng¹, Lingjie Zhang¹, Songhua Fang²

¹Department of Radiology, Sir Run Run Shaw Hospital, Zhejiang University School of Medicine, Hangzhou 310016, Zhejiang Province, China; ²Department of Radiology, Zhejiang Provincial People's Hospital, People's Hospital of Hangzhou Medical College, Hangzhou 310014, Zhejiang Province, China

Received November 21, 2019; Accepted April 25, 2020; Epub June 15, 2020; Published June 30, 2020

Abstract: This article aimed to investigate the CT and MRI features of G1 and G2 pancreatic neuroendocrine tumors (NETs) and to provide evidence for clinical treatment. Forty-three patients with pancreatic neuroendocrine neoplasms (pNENs) confirmed by surgical pathology were enrolled. The CT and MRI features were analyzed and the data were processed using SPSS 19.0 statistical software package. Because this was a retrospective study, exemption from informed consent was applied. Of the 43 patients with pNENs, 40 had single lesions and 3 had multiple lesions. A total of 52 lesions were observed, and the largest diameter of a single tumor ranged from 7 to 153 mm, with an average diameter of 39.9 mm. The difference between the maximum diameter of G1 and G2 NETs was statistically significant ($P < 0.05$). There were significant differences in the boundary and enhancement characteristics between G1 and G2 NETs ($P < 0.01$), but no statistically significant difference in the change in pancreatic contour ($P > 0.05$). Compared with G1 NETs, G2 NETs were more significant, but had blurred borders and an uneven density after enhancement. These lesions were more prone to calcification, cystic necrosis and pancreatic duct dilatation. Also, peripancreatic tissue or vascular invasion, lymphadenopathy and distant metastasis were only found in G2 NETs. At last, G1 and G2 NETs can be discriminated based on lesion size, border, enhancement characteristics, surrounding tissue or vascular invasion, lymphadenopathy and distant metastasis. CT and MRI can complement each other and further improve the diagnosis of pNENs.

Keywords: Pancreatic neuroendocrine neoplasms, pancreatic neuroendocrine tumours, computed tomography, magnetic resonance imaging

Introduction

Pancreatic neuroendocrine neoplasms (pNENs) are rare tumors that originate in pancreatic endocrine cells and have an incidence of about one in 100,000; accounting for only 1%-2% of all pancreatic tumors [1]. In the SEER 18 registry grouping (2000-2012) the highest incidence rates were 1.49 per 100,000 in the lung, 3.56 per 100,000 in gastroenteropancreatic sites, and 0.84 per 100,000 in NETs with an unknown primary site [2]. The incidence of pNENs has risen rapidly in the last 20 years, which may be related to the increased use of CT, MRI, ultrasonography and endoscopy [3]. Functional pNENs include insulinoma, gastrinoma, glucagonoma, and vasoactive intestinal peptide tumors. Non-functional pNENs have no clinical endocrine symptoms. The biological behavior of pNENs is

challenging to predict from histological features and there are many histopathological grading systems [4]. In 2017, the World Health Organization (WHO) classified pNENs not only by their mitotic count and the proliferation index with Ki-67 expression, but also by their morphological features. These include the presence of a well-differentiated pancreatic neuroendocrine tumour (NET) rated G1, G2, or G3 and poorly differentiated neuroendocrine carcinoma (NEC), dividing NEC G3 into NET G3 and NEC G3 according to WHO in 2017 [5]. The 2017 classification now also recognizes well differentiated G3 NETs, which generally have an Ki-67 index between 20% and 50% [6].

The management of patients with pNENs is multidisciplinary and often multimodal [7]. One of the essential aspects to tailor the optimal

treatment for pNENs patients is tumor grading. NECs are known to be histologically and genetically different from NETs, and they require different therapeutic strategies [8]. Patients with well-differentiated pNENs are usually managed with somatostatin analogues and further treatment such as surgery or peptide receptor radionuclide therapy (PRRT) can be considered [9, 10]. Patients with poorly differentiated NEC should be treated with platinum-based systemic chemotherapy [11]. Although G1 and G2 NET are generally treated as the same entity, there are some differences in the treatment strategies of the two in clinical practice [12]. So, accurate preoperative assessment of grading and prognosis are important for selecting treatment options. At present, sporadic reports about the preoperative grading of pNENs using CT and magnetic resonance (MR) can be found [13]. Studies have shown that the morphological characteristics of pNENs may affect their biological behavior, as the blood supply and enhancement of tumors are related to histological grade and prognosis [14].

This study retrospectively analyzed 43 patients with pNENs confirmed by surgical pathology in our hospital. The preoperative CT and MRI data were used to distinguish the imaging features of G1 and G2 NET.

Materials and methods

General data

Forty-three patients, 21 males and 22 females, aged 22-71 years (mean age 50.98 years) with pNENs confirmed by surgical pathology in our hospital from 2015 to 2018, were enrolled in this study. Twenty-eight patients underwent CT examination, two underwent MRI examination (only MRI plain scan, no enhanced scan), and 13 patients underwent simultaneous CT and MRI. CT and MRI examination sequences were in no particular order. The approval number of the institutional review board of Sir Run Run Shaw Hospital was 20181106-22. Because the data of this study was retrospective the exemption of informed consent was applied.

Pathological grading standards

In 2017, the World Health Organization (WHO) classified pNENs into grades NET G1, G2, G3 and NEC G3 based on mitotic count and the

Ki-67 index as follows: NET G1: a mitotic count $<2/10$ under high power fields and/or Ki-67 $\leq 2\%$; NET G2: mitotic count 2-20/10 under high power fields and/or Ki-67 3%-20%; and NET/NEC G3: mitotic count $>20/10$ under high power fields and/or Ki-67 $>20\%$.

Clinical manifestations

Eight patients had paroxysmal dizziness, fatigue, palpitations, cold sweats, syncope with increased serum insulin, and decreased fasting blood glucose. Two patients had diabetes with increased serum glucagon. Patients with non-functional pNENs had different degrees of upper abdominal discomfort, pain and weight loss, and a pancreatic mass or liver mass was found during physical examination.

Imaging examinations

In CT examination, GE Hispeed CT/i and Siemens Somatom Sensation 16 CT systems were used. The patients fasted for more than 8 h before the examination and mannitol 13.75 g plus 500 mL of water was given 30 min before the CT scan to fill the stomach and duodenum. The scanning voltage was 120 kV and the tube current was 150 mA. The patients underwent plain and enhanced scanning. The conventional plain scanning was performed on the upper abdomen, the layer thickness was 3-5 mm. The iodine contrast agent used was Ultravist or Omnipaque and the total dose was 70-100 mL. A high-pressure syringe was used for rapid, large-dose injection at a single injection rate of 3 ml/s. Two-stage (arterial and portal venous) scans were used. The arterial and portal venous phases were scanned at 25 s and 65 s after rapid injection of contrast agent, respectively. The scanning range of the arterial phase mainly covered the pancreas. The thickness of the layer was 2.5-5 mm and the pitch was 1-1.2 mm. The scanning range of the portal venous phase included the pancreas and the liver. The thickness was increased to 5 mm and the pitch was 1.5 mm. During the scanning, the patients were required to hold their breath in a calm state to avoid movement of the scanning plane and the generation of artifacts. Surface shaded display (SSD), maximum intensity projection (MIP), multiplanar reconstruction (MPR) and three-dimensional vascular reconstruction were applied partially to show the relationship between tumor and blood vessels.

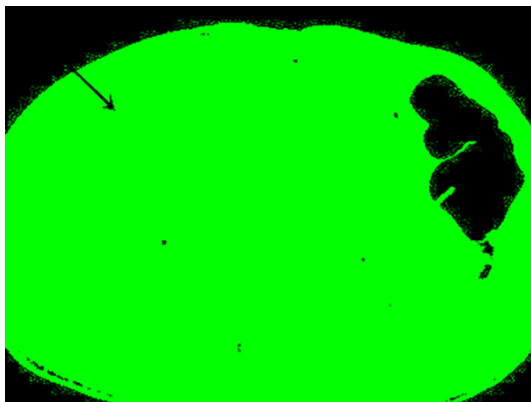


Figure 1. Multiple G2 pNETs lesions (white arrow), mildly dilated pancreatic duct and hepatic metastases (black arrow).

MRI examination

A GE 1.5T superconducting magnetic resonance scanner was used. The patients fasted for more than eight hours before scanning. Mannitol 13.75 g plus 500 ml of water was given 30 min before the scanning to fill the stomach and duodenum. A phased-array surface coil (TORSO) was used to scan from the dome to the lower edge of the liver. The sequence included: (1) conventional spin-echo (SE) sequence T1-weighted image (T1WI), T2WI; (2) fat suppression T2WI (FS-T2WI), layer thickness 8 mm, layer spacing 2 mm, and matrix 256×160; (3) fast spoiled gradient echo (FSPGR) sequence T1 double echo scan; (4) FSPGR sequence for pancreatic enhancement scan; and (5) liver acquisition with volume acceleration (LAVA) sequence for pancreatic enhancement scan (partial replacement for FSPGR sequence). The contrast agent, Gd-DTPA, was injected intravenously with a high-pressure syringe at a dose of 12-15 ml, an injection rate of 3 ml/s, in the arterial phase (25 s), portal venous phase (65 s) and delayed phase (180 s). Each phase was scanned once to obtain a dynamic, enhanced image of the pancreas. The enhanced scanning layer thickness was 5 mm, the layer spacing was 1 mm and the matrix was 256×160.

Image evaluation

Two doctors with experience in abdominal imaging diagnosis independently analyzed the patients' CT and MRI features. They were blinded to the patients' medical history and pathological results. When the findings of the two doctors were inconsistent, they were discussed

until a unanimous decision was reached. CT and MRI findings of tumor location, number, size, border, pancreatic contour change and enhancement characteristics were explicitly analyzed. Pancreatic contour change was divided into two types: intrapancreatic growth (the lesion was confined to the pancreas and the shape of the pancreas was normal) and extrapancreatic growth. The degree of enhancement of the tumor was divided into three types: obvious, moderate and mild. Obvious enhancement was higher than pancreas enhancement in the portal phase; moderate enhancement was similar to pancreas enhancement in the portal phase; mild enhancement was lower than pancreas enhancement in the portal phase. According to whether there were low enhancement or no enhancement areas in the lesion, enhancement form was divided into two types: uniform enhancement and uneven enhancement.

Statistical analysis

To compare the difference in diameter between G1 and G2 NET, an independent sample t-test was performed using SPSS 19.0 statistical software package if both Normal Distribution and Homogeneity of Variance were satisfied. $P < 0.05$ was considered statistically significant. A comparison was made between G1 and G2 NET in terms of pancreatic contour change, whether the boundary between the lesion and surrounding pancreatic tissue was clear, and whether the enhancement was uniform using the Chi-square test with SPSS 19.0 statistical software package, $P < 0.05$ was considered statistically significant.

Results

All patients were confirmed to have pNENs by surgical pathology. According to the WHO classification (2017), 18 patients had G1 NETs, and 25 patients had G2 NETs. The pNENs were located in the pancreatic head in 19 patients, in the pancreatic body in 6 patients, in the pancreatic tail in 11 patients, in the pancreatic head and body in 1 patient, in the pancreatic body and tail in 5 patients, and in all parts of the pancreas in 1 patient. Forty patients had single lesions and 3 had multiple lesions. Two of these patients had two lesions in the pancreas, all of which were G1 NETs. One patient had eight lesions in the pancreas, which were all G2 NETs (**Figures 1, 2**). A total of 52 lesions

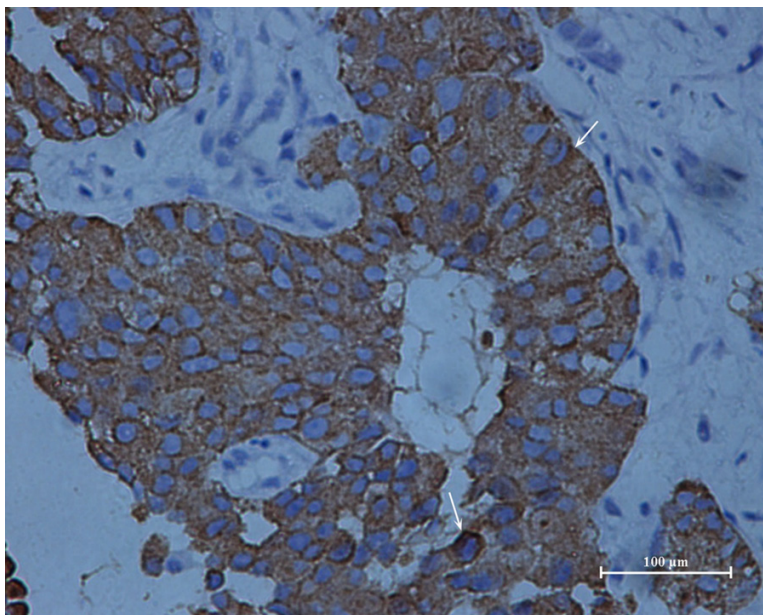


Figure 2. Multiple G2 pNETs immunohistochemistry displayed positive staining (arrow) (CgA×400).

Table 1. Comparison of imaging characteristics between 20 G1 NET lesions and 32 G2 NET lesions

CT and MRI features	G1 NET	G2 NET	χ^2	<i>P</i>
Intrapancreatic growth	11	25	3.090	>0.05
Extrapancreatic growth	9	7		
Well-defined	17	7	19.734	<0.01
Ill-defined	3	25		
Uniform enhancement	14	7	10.728	<0.01
Uneven enhancement	6	23		

Note: The unit of lesion is one; 2 patients only underwent MRI plain scanning, but not enhanced scanning.

were identified, the maximum in-plane diameter of a single tumor ranged from 7 to 153 mm, with an average diameter of 39.9 mm. In the 18 patients with G1 NETs, 20 lesions were observed with a maximum diameter of 8-75 mm and an average diameter of 27.5 mm. In the 25 patients with G2 NETs, 32 lesions were observed with a maximum diameter of 7-153 mm and an average diameter of 47.7 mm. The difference between the maximum diameter of G1 and G2 NETs was statistically significant ($P<0.05$).

There were significant differences in the boundary and enhancement characteristics between G1 and G2 NETs ($P<0.01$), but no statistically significant change in pancreatic contour

($P>0.05$). The imaging characteristics of the patients are shown in **Table 1**.

Compared with G1 NETs, G2 NETs were large, lobulated, or irregular with blurred borders and an uneven density after enhancement. They were also more prone to calcification, cystic necrosis and pancreatic duct dilatation. Seven patients with G2 NETs had calcification, nine patients had mild common bile duct and pancreatic duct dilatation, two patients had complete cystic changes around the lesions and one patient had cystic-solid changes with a nodular ring-like-enhanced cyst wall (**Figure 3**). In addition, peripancreatic tissue, vascular invasion, lymphadenopathy and distant metastasis were only found in G2 NETs (**Figure 1**). MPR and three-dimensional vascular reconstruction were applied partially to show the relationship between tumors, blood vessels and surrounding structures (**Figures 4, 5**).

In this study, two G1 NETs were not detected by CT. The smaller tumors in the pancreas did not cause pancreatic contour changes, and the tumors showed uniform density on CT plain scan and enhanced scan, similar to pancreatic parenchyma. The lesions showed a low signal change relative to pancreatic parenchyma in the MR T1W lipid-inhibiting sequence (**Figure 6**) and LAVA dynamic enhancement of the arterial phase showed moderate enhancement. Preoperative CT did not diagnose one patient with multiple G1 NETs. Retrospective readings showed exogenous tumors protruding from the surface of the pancreas, similar to the nodular gland structure protruding from the surface of the pancreas. MRI plain scan showed the long T1 and long T2 signal nodules, which were enhanced following contrast administration.



Figure 3. Cystic G2 pNET with the cystic wall of the pancreatic tail showing nodular and ring-like enhancement in the FSPGR dynamic enhanced scan (arrow).



Figure 4. G2 pNET with a cupping edge (black arrow) between the tumor and pancreas in MPR with invasion of the spleen and left kidney (white arrow).

Discussion

Pancreatic neuroendocrine neoplasms (pNENs) are rare, which develop from the embryonic neuroectoderm and are part of the gastrointestinal neuroendocrine tumors. All pNENs are

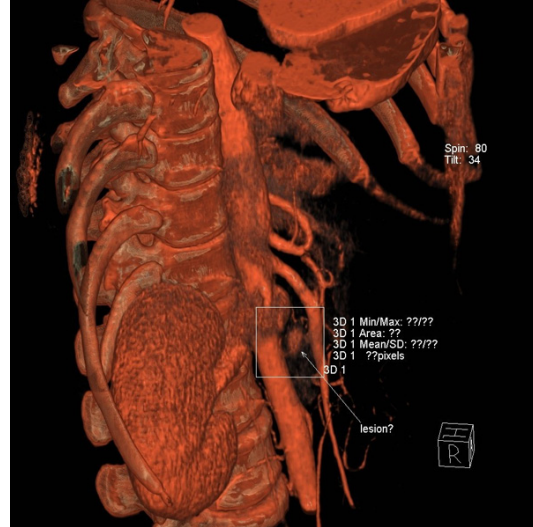


Figure 5. An enhanced G1 pNET nodule in three-dimensional vascular reconstruction (arrow).

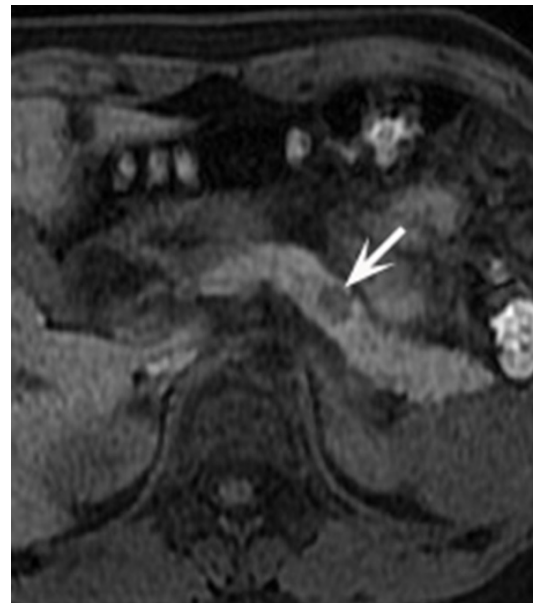


Figure 6. G1 pNET hypointense lesion in T1WI with fat saturation (arrow).

potentially malignant but differ in the likelihood of invasive behavior or metastasis, and the classification of pNENs is closely related to patient survival [15]. Histological diagnosis of pNENs is based on morphological and immunohistochemical features, including the expression of chromogranin A (CgA), synaptophysin (Syn), CD56, and Ki-67. In 2017, the updated WHO classification for pNENs divided NENs into G1, G2, G3 neuroendocrine tumor (NET) and neuroendocrine carcinoma (NEC) based on the

histological differentiation, including the Ki-67 proliferation index and the mitotic rate [16]. In fact, the full immune profiles in the epithelial region were strongly associated with their histological classifications, and the NET grading could be further distinguished between G1, G2, and G3 using the CD3+/PD-1 and CD204+/PD-L1 features [17]. Adoption of the WHO unified terminology and grading system is the first step in the diagnosis of pNENs, which provides a safe, scientific background and development basis for the advancement of relevant treatment modalities. This study focused on analyzing the relationship between CT and MRI findings and pathological grades of pNENs, which provided some useful information for clinical treatment strategies and the prediction of disease prognosis.

The results of this study suggest that there are differences in imaging features between G1 NETs and G2 NETs. Previous studies have shown that solid tumors ≥ 3 cm in diameter are usually non-benign, while 30% of tumors < 3 cm in diameter can be malignant [18]. This study showed that there is a correlation between maximum tumor diameter and grade. The maximum tumor diameter in the G1 group was 27.5 mm, and the maximum tumor diameter in the G2 group was 47.7 mm. The difference between the two groups was statistically significant, suggesting that G2 tumors are more likely to be larger. It is worth noting that previous studies have shown that tumor diameter is related to the survival rate [19], and tumor diameter is an important parameter affecting pancreatic resection [20].

G1 NETs have an abundant blood supply. They are generally small in size and more solid. Plain scans usually show low-density and the tumor boundaries are clear, sometimes highlighting the pancreatic margin. A tumor in the arterial phase is often uniformly enhanced and the tumor in the venous phase can be continuously enhanced or have equal density. Therefore, detection in the arterial phase is vital [21]. Nevertheless, small pNETs can also sometimes be detected during the portal phase because of their greater attenuation compared to the surrounding pancreatic parenchyma [22]. The specific clinical symptoms are essential for diagnosis. Some G1 NETs of small size cannot be detected by a single imaging method, and other imaging methods should be used.

When G2 NETs are identified clinically, the tumor is large and often shows low density or mixed low-density changes during the plain scan. Larger pNETs often have irregular contrast enhancement due to areas of necrosis. The boundary is unclear and calcification, necrosis and cystic changes are seen in the central part of the tumor. Calcifications and cystic elements are present in approximately 15% and 30% of cases, respectively [23]. Although calcification is uncommon in pNENs, almost 100% of these tumors suggest a risk of non-benign biological behavior [24]. The solid part of the cystic-solid lesion is also rich in blood supply, which may show markedly uneven or ring-like enhancement in the arterial phase. Some of the apparent enhancement in the portal venous phase may be related to the expansion of the tumor vessels and retention of the contrast agent in the tumor. Contrast uptake as visualized by CT is another criteria, appearing to be slower in less well-differentiated tumors [25]. Complete cystic changes are rare and can consist of one cyst or multiple cysts, and are mainly from tumor hemorrhage or necrosis. MRI has unique advantages as it can show specific components such as cystic changes, hemorrhage and envelope structure.

Metastasis or infiltration of surrounding organs and tissues is also an important factor for identifying G1 and G2 NETs, as the WHO (2017) pathological grading criteria for pNENs is based on mitotic count and the Ki-67 index, which may reflect the proliferation and invasiveness of tumor cells. The lower the degree of tumor differentiation, the higher the pathological grade and the higher the tumor proliferation and invasiveness. The advantages of CT and MRI are that they can simultaneously detect peripancreatic tissue or vascular invasion, lymphadenopathy and distant metastasis of G2 NETs. Liver metastases also have a rich blood supply and staged scans are valuable in their detection. Preoperative vascular invasion, main pancreatic duct dilatation, peripancreatic lymph node enlargement and distant metastasis not only predict uncertain or invasive biological behavior, but are also strongly associated with poor long-term prognosis.

In terms of tumor detection, magnetic resonance T2WI showed that the lesion generally has a high signal, and T2WI showed that the signal is low if collagen and fibrous tissue are

included. On the T1WI lipid-inhibiting sequence (FSPGR sequence containing fat-suppressed T1WI), normal pancreas tissues showed a high signal due to abundant water-like proteins, while tumor tissues showed a low signal without water-like proteins, with the signal difference between the two [26]. The value of the T1WI lipid-inhibiting sequence was identified, while CT scans did not show the lesions with similar density to pancreatic parenchyma. MRI has good sensitivity for detecting pancreatic NETs, especially those measuring more than 2 cm [27]. Whole-body MRI also improves the detection of distant lesions that have an impact on management [28]. Thus, we believe that MRI has higher sensitivity and specificity than CT.

This group of patients confirmed that the growth pattern of pNENs is different from that of pancreatic cancer, and the former shows swelling and is exogenous. There was no significant difference in the changes in pancreatic contour between G1 NETs and G2 NETs. If G1 NETs are located near tissues and blood vessels, they are not directly invaded and can often be surgically removed. If G2 NETs grow large, they directly invade the surrounding tissues and blood vessels. In the absence of periductal infiltration and neurotropic growth, there is no apparent involvement of the pancreatic duct and bile duct or only mild dilatation caused by compression. However, due to the characteristics of periductal infiltration and neurotropic growth, pancreatic cancer often invades the pancreatic duct and/or common bile duct, causing prominent dilatation of the pancreatic duct and/or common bile duct, pancreatic atrophy and clinical symptoms such as indigestion and jaundice.

Also, pNENs with exogenous growth are often relatively large and need to be differentiated from stromal tumors of the gastrointestinal tract, peritoneal and retroperitoneal neurogenic tumors and extra-adrenal pheochromocytoma. Preoperative diagnostic errors were observed in 2 patients with G2 NETs. Preoperative CT diagnosis was a malignant spleen tumor that had invaded the tail of the pancreas. The postoperative analysis was performed mainly due to the exogenous growth of these tumors, the large mass and the main body located in the spleen leading to misdiagnosis. In our experience, a cup-like change at the interface

between the tumor and the pancreatic margin and changes in the large blood vessels around the pancreas can help to diagnose pancreatic-derived tumors.

Some tumors were not detected as their degree of enhancement was consistent with blood vessels, and were thus mistaken as part of the blood vessels. These tumors were similar in size and shape to adjacent blood vessels. With the emergence of multi-slice spiral CT (MSCT), pancreas high-resolution multi-phase scanning is possible. The application of CT angiography, three-dimensional vascular reconstruction, MIP, MPR, SSD and other post-processing software can clearly judge the spatial relationship between tumors, blood vessels, and surrounding structures. According to Foti, MSCT is superior to MRI in the preoperative evaluation of vascular involvement of pNENs [29]. Therefore, MSCT should be considered as a preoperative imaging tool for non-functional pNENs.

In summary, this study analyzed the imaging findings of G1 NETs and G2 NETs. The discriminating factors in these two types of pNENs included lesion size, boundary, enhancement characteristics, surrounding tissue or vascular invasion, lymph node enlargement and distant metastasis. Besides, the spatial resolution and density resolution of CT were higher than those of MRI, and the soft tissue resolution of MRI was higher than that of CT. CT and MRI can complement each other and further improve the diagnosis of pNENs. Our study was retrospective and almost based on morphological research which was multifarious and inconvenient in application. Small number of patients is another limitation. In the future, more prospective cohort studies with quantitative parameters in a larger group of patients will be used to grade pNENs and characterize lesions, such as contrast uptake by dynamic enhanced CT, the apparent diffusion coefficient (ADC) value of MRI.

Acknowledgements

Project supported by the Zhejiang Medical Science and Technology Project Foundation (2015KYA134).

Disclosure of conflict of interest

None.

Pancreatic neuroendocrine neoplasms: a correlative study

Address correspondence to: Dr. Songhua Fang, Department of Radiology, Zhejiang Provincial People's Hospital, People's Hospital of Hangzhou Medical College, Hangzhou 310014, Zhejiang Province, China. E-mail: fsh@hmc.edu.cn

References

- [1] Buetow PC, Miller DL, Parrino TV and Buck JL. Islet cell tumors of the pancreas: clinical, radiologic, and pathologic correlation in diagnosis and localization. *Radiographics* 1997; 17: 453-472; quiz 472A-472B.
- [2] Dasari A, Shen C, Halperin D, Zhao B, Zhou S, Xu Y, Shih T and Yao JC. Trends in the incidence, prevalence, and survival outcomes in patients with neuroendocrine tumors in the United States. *JAMA Oncol* 2017; 3: 1335-1342.
- [3] Yao JC, Hassan M, Phan A, Dagohoy C, Leary C, Mares JE, Abdalla EK, Fleming JB, Vauthey JN, Rashid A and Evans DB. One hundred years after "carcinoid": epidemiology of and prognostic factors for neuroendocrine tumors in 35,825 cases in the United States. *J Clin Oncol* 2008; 26: 3063-3072.
- [4] Ferrone CR, Tang LH, Tomlinson J, Gonen M, Hochwald SN, Brennan MF, Klimstra DS and Allen PJ. Determining prognosis in patients with pancreatic endocrine neoplasms: can the WHO classification system be simplified? *J Clin Oncol* 2007; 25: 5609-5615.
- [5] Takahashi D, Kojima M, Suzuki T, Sugimoto M, Kobayashi S, Takahashi S, Konishi M, Gotohda N, Ikeda M, Nakatsura T, Ochiai A and Nagino M. Profiling the tumour immune microenvironment in pancreatic neuroendocrine neoplasms with multispectral imaging indicates distinct subpopulation characteristics concordant with WHO 2017 classification. *Sci Rep* 2018; 8: 13166.
- [6] Heetfeld M, Chougnat CN, Olsen IH, Rinke A, Borbath I, Crespo G, Barriuso J, Pavel M, O'Toole D and Walter T. Characteristics and treatment of patients with G3 gastroenteropancreatic neuroendocrine neoplasms. *Endocr Relat Cancer* 2015; 22: 657-664.
- [7] Pavel M, O'Toole D, Costa F, Capdevila J, Gross D, Kianmanesh R, Krenning E, Knigge U, Salazar R, Pape UF and Oberg K. ENETS consensus guidelines update for the management of distant metastatic disease of intestinal, pancreatic, bronchial neuroendocrine neoplasms (NEN) and NEN of unknown primary site. *Neuroendocrinology* 2016; 103: 172-185.
- [8] Tang LH, Basturk O, Sue JJ and Klimstra DS. A practical approach to the classification of WHO Grade 3 (G3) well-differentiated neuroendocrine tumor (WD-NET) and poorly differentiated neuroendocrine carcinoma (PD-NEC) of the pancreas. *Am J Surg Pathol* 2016; 40: 1192-1202.
- [9] Crippa S, Partelli S, Bassi C, Berardi R, Capelli P, Scarpa A, Zamboni G and Falconi M. Long-term outcomes and prognostic factors in neuroendocrine carcinomas of the pancreas: morphology matters. *Surgery* 2016; 159: 862-871.
- [10] Fazio N and Milione M. Heterogeneity of grade 3 gastroenteropancreatic neuroendocrine carcinomas: new insights and treatment implications. *Cancer Treat Rev* 2016; 50: 61-67.
- [11] Crippa S, Partelli S, Belfiori G, Palucci M, Muffatti F, Adamenko O, Cardinali L, Doglioni C, Zamboni G and Falconi M. Management of neuroendocrine carcinomas of the pancreas (WHO G3): a tailored approach between proliferation and morphology. *World J Gastroenterol* 2016; 22: 9944-9953.
- [12] Zhao W, Quan Z, Huang X, Ren J, Wen D, Zhang G, Shi Z, Yin H and Huan Y. Grading of pancreatic neuroendocrine neoplasms using pharmacokinetic parameters derived from dynamic contrast-enhanced MRI. *Oncol Lett* 2018; 15: 8349-8356.
- [13] Kim DW, Kim HJ, Kim KW, Byun JH, Song KB, Kim JH and Hong SM. Neuroendocrine neoplasms of the pancreas at dynamic enhanced CT: comparison between grade 3 neuroendocrine carcinoma and grade 1/2 neuroendocrine tumour. *Eur Radiol* 2015; 25: 1375-1383.
- [14] Tatsumoto S, Kodama Y, Sakurai Y, Shinohara T, Katanuma A and Maguchi H. Pancreatic neuroendocrine neoplasm: correlation between computed tomography enhancement patterns and prognostic factors of surgical and endoscopic ultrasound-guided fine-needle aspiration biopsy specimens. *Abdom Imaging* 2013; 38: 358-366.
- [15] Sellner F, Thalhammer S, Stattner S, Karner J and Klimpfner M. TNM stage and grade in predicting the prognosis of operated, non-functioning neuroendocrine carcinoma of the pancreas—a single-institution experience. *J Surg Oncol* 2011; 104: 17-21.
- [16] Kim JY, Hong SM and Ro JY. Recent updates on grading and classification of neuroendocrine tumors. *Ann Diagn Pathol* 2017; 29: 11-16.
- [17] Kim ST, Ha SY, Lee S, Ahn S, Lee J, Park SH, Park JO, Lim HY, Kang WK, Kim KM and Park YS. The impact of PD-L1 expression in patients with metastatic GEP-NETs. *J Cancer* 2016; 7: 484-489.
- [18] Gallotti A, Johnston RP, Bonaffini PA, Ingkakul T, Deshpande V, Fernández-del Castillo C and Sahani DV. Incidental neuroendocrine tumors of the pancreas: MDCT findings and features of malignancy. *AJR Am J Roentgenol* 2013; 200: 355-362.

Pancreatic neuroendocrine neoplasms: a correlative study

- [19] Bettini R, Partelli S, Boninsegna L, Capelli P, Crippa S, Pederzoli P, Scarpa A and Falconi M. Tumor size correlates with malignancy in non-functioning pancreatic endocrine tumor. *Surgery* 2011; 150: 75-82.
- [20] Falconi M, Zerbi A, Crippa S, Balzano G, Boninsegna L, Capitanio V, Bassi C, Di Carlo V and Pederzoli P. Parenchyma-preserving resections for small nonfunctioning pancreatic endocrine tumors. *Ann Surg Oncol* 2010; 17: 1621-1627.
- [21] Procacci C, Carbognin G, Accordini S, Biasiutti C, Bicego E, Romano L, Guarise A, Minniti S, Pagnotta N and Falconi M. Nonfunctioning endocrine tumors of the pancreas: possibilities of spiral CT characterization. *Eur Radiol* 2001; 11: 1175-1183.
- [22] Sundin A, Arnold R, Baudin E, Cwikla JB, Eriksson B, Fanti S, Fazio N, Giammarile F, Hicks RJ, Kjaer A, Krenning E, Kwekkeboom D, Lombard-Bohas C, O'Connor JM, O'Toole D, Rockall A, Wiedenmann B, Valle JW and Vullierme MP. ENETS consensus guidelines for the standards of care in neuroendocrine tumors: radiological, nuclear medicine & hybrid imaging. *Neuroendocrinology* 2017; 105: 212-244.
- [23] Toshima F, Inoue D, Komori T, Yoshida K, Yoneda N, Minami T, Matsui O, Ikeda H and Gabata T. Is the combination of MR and CT findings useful in determining the tumor grade of pancreatic neuroendocrine tumors? *Jpn J Radiol* 2017; 35: 242-253.
- [24] Rha SE, Jung SE, Lee KH, Ku YM, Byun JY and Lee JM. CT and MR imaging findings of endocrine tumor of the pancreas according to WHO classification. *Eur J Radiol* 2007; 62: 371-377.
- [25] Lotfalizadeh E, Ronot M, Wagner M, Cros J, Couvelard A, Vullierme MP, Allaham W, Hentic O, Ruzniewski P and Vilgrain V. Prediction of pancreatic neuroendocrine tumour grade with MR imaging features: added value of diffusion-weighted imaging. *Eur Radiol* 2017; 27: 1748-1759.
- [26] Moore NR, Rogers CE and Britton BJ. Magnetic resonance imaging of endocrine tumours of the pancreas. *Br J Radiol* 1995; 68: 341-347.
- [27] Deguelte S, de Mestier L, Hentic O, Cros J, Lebtahi R, Hammel P and Kianmanesh R. Preoperative imaging and pathologic classification for pancreatic neuroendocrine tumors. *J Visc Surg* 2018; 155: 117-125.
- [28] Moryoussef F, de Mestier L, Belkebir M, Deguelte-Lardiere S, Brixi H, Kianmanesh R, Hoefel C and Cadiot G. Impact of liver and whole-body diffusion-weighted MRI for neuroendocrine tumors on patient management: a pilot study. *Neuroendocrinology* 2017; 104: 264-272.
- [29] Foti G, Boninsegna L, Falconi M and Mucelli RP. Preoperative assessment of nonfunctioning pancreatic endocrine tumours: role of MDCT and MRI. *Radiol Med* 2013; 118: 1082-1101.